



# The Population Pharmacokinetics of High-Dose Methotrexate in Infants with Acute Lymphoblastic Leukemia Highlight the Need for Bedside Individualized Dose Adjustment: A Report from the Children's Oncology Group

Ryan J. Beechinor<sup>1</sup> · Patrick A. Thompson<sup>2</sup> · Michael F. Hwang<sup>1</sup> · Ryan C. Vargo<sup>3</sup> · Lisa R. Bomgaars<sup>4</sup> · Jacqueline G. Gerhart<sup>1</sup> · ZoAnn E. Dreyer<sup>4</sup> · Daniel Gonzalez<sup>1</sup>

Published online: 27 February 2019  
© Springer Nature Switzerland AG 2019

## Abstract

**Background** Infants with acute lymphoblastic leukemia (ALL) treated with high-dose methotrexate may have reduced methotrexate clearance (CL) due to renal immaturity, which may predispose them to toxicity.

**Objective** The aim of this study was to develop a population pharmacokinetic (PK) model of methotrexate in infants with ALL.

**Methods** A total of 672 methotrexate plasma concentrations were obtained from 71 infants enrolled in the Children's Oncology Group (COG) Clinical Trial P9407. Infants received methotrexate 4 g/m<sup>2</sup> intravenously for four cycles during weeks 4–12 of intensification. A population PK analysis was performed using NONMEM<sup>®</sup> version 7.4. The final model was evaluated using a non-parametric bootstrap and a visual predictive check. Simulations were performed to evaluate methotrexate dose and the utility of a bedside algorithm for dose individualization.

**Results** Methotrexate was best characterized by a two-compartment model with allometric scaling. Weight was the only covariate included in the final model. The coefficient of variation for interoccasion variability (IOV) on CL was relatively high at 25.4%, compared with the interindividual variability for CL and central volume of distribution (10.7% and 13.2%, respectively). Simulations identified that 21.1% of simulated infants benefitted from bedside dose adjustment, and adjustment of methotrexate doses during infusions can avoid supratherapeutic concentrations.

**Conclusion** Infants treated with high-dose methotrexate demonstrated a relatively high degree of IOV in methotrexate CL. The magnitude of IOV in the CL of methotrexate suggests that use of a bedside algorithm may avoid supratherapeutic methotrexate concentrations resulting from high IOV in methotrexate CL.

**Electronic supplementary material** The online version of this article (<https://doi.org/10.1007/s40262-018-00734-0>) contains supplementary material, which is available to authorized users.

✉ Daniel Gonzalez  
daniel.gonzalez@unc.edu

- <sup>1</sup> Division of Pharmacotherapy and Experimental Therapeutics, UNC Eshelman School of Pharmacy, The University of North Carolina at Chapel Hill, CB #7569, Chapel Hill, NC 27599-7569, USA
- <sup>2</sup> University of North Carolina Lineberger Comprehensive Cancer Center, Chapel Hill, NC, USA
- <sup>3</sup> Pharmacokinetics, Pharmacodynamics, and Drug Metabolism, Merck & Co., Inc., Kenilworth, NJ, USA
- <sup>4</sup> Texas Children's Cancer and Hematology Center, Baylor College of Medicine, Houston, TX, USA

## Key Points

High-dose methotrexate is a crucial component of treatment protocols for acute lymphoblastic leukemia (ALL), but few studies have characterized its disposition in infants.

Infants with ALL demonstrated significant interoccasion variability in their clearance of methotrexate across treatment cycles.

Monte Carlo simulations performed using a developed population pharmacokinetic model revealed the utility of bedside monitoring and dose adjustment to optimize methotrexate exposure.

## 1 Introduction

Acute lymphoblastic leukemia (ALL) is the most common form of pediatric cancer, representing 25% of all cancers diagnosed in children under 15 years of age [1, 2]. Over the past several decades there have been significant improvements in the prognosis of pediatric ALL, and 5-year overall survival for contemporary treatment protocols has approached 90% [3]. Despite this improvement, the outcomes of infants diagnosed at < 1 year of age have been consistently worse [4]. The explanation for this lack of improvement in the clinical outcomes of infant ALL has not been fully elucidated; however, there are features of infant ALL thought to be responsible for its poor prognosis, including both the greater frequency of high-risk genetic mutations as well as higher tumor burden at presentation [5–7]. In addition to these factors, physiological differences between infants and older children may lead to alterations in drug disposition and pharmacokinetics (PK) of chemotherapy that may affect infant outcomes. This has led to the development of infant-specific protocols designed to increase the intensity of therapy in these subjects [3, 4, 7].

Methotrexate is an antineoplastic agent used commonly in a variety of childhood malignancies, and is a crucial component to ALL treatment protocols [8, 9]. Methotrexate is a folate analog that competitively inhibits the activity of dihydrofolate dehydrogenase (DHFR), causing depletion of purines and thymidylate, which halts DNA synthesis causing cell death [10, 11]. This effect is amplified in rapidly dividing cells, leading to S-phase-specific cytotoxicity of methotrexate [8]. Due to the high expression of DHFR in ALL cells, high-dose methotrexate is one therapeutic strategy utilized to saturate DHFR and maximize cytotoxicity [12, 13]. However, high-dose methotrexate requires both therapeutic drug monitoring (TDM) and significant supportive care to avoid excessive exposure to methotrexate, which has been shown to cause nephrotoxicity, myelotoxicity, mucositis, neurological complications, and other adverse effects [14, 15].

Based on the physiologic differences between infants and older children, the PK of methotrexate in infants may be altered due to several factors. First, methotrexate is primarily eliminated by renal excretion, as adult studies have shown that approximately 70–90% of each dose is excreted unchanged in urine [15, 16]. Infants are known to have both delayed and variable maturation of renal tubule function, glomerular filtration rate, and renal blood flow [17–20]. Therefore, elimination of methotrexate in younger infants may be significantly delayed compared with older children, which could increase toxicity. Additionally, methotrexate is known to have delayed

elimination in patients with extracellular fluid accumulations [14]. This may affect drug disposition in infants, who are known to undergo significant changes in total body water content from approximately 75% during the neonatal period to 55% in adulthood [21, 22].

Despite these concerns, to date there are limited published PK analyses describing the disposition of methotrexate in this vulnerable patient population. Moreover, few studies have included infants < 6 months of age when these physiological changes are most relevant, and none have used population PK to characterize the disposition of methotrexate in this patient population [21, 23, 24]. The use of population PK offers several unique advantages over conventional PK analyses, most notably the ability to quantify the effects of patient covariates on drug exposure using sparse PK sampling [25–27]. A non-compartmental analysis with a portion of the data used for the current study was previously published [28], but a population PK analysis has not been previously performed. The objectives of this study were to develop a population PK model of methotrexate in infants with ALL, to characterize the impact of interoccasion variability (IOV) on this model, and to use simulations to evaluate the impact of various doses on methotrexate exposure.

## 2 Methods

### 2.1 Patient Population

Methotrexate concentrations were obtained from infants enrolled in the Children's Oncology Group (COG) Clinical Trial P9407, a portion of whom were enrolled in a PK sub-study. The details of the study design, inclusion and exclusion criteria, treatment protocol, and PK sampling have been described previously [28]. Briefly, this study included subjects with newly diagnosed ALL < 366 days postnatal age (PNA) and > 36 weeks gestational age at birth with congenital ALL. Exact dates of infusions were not available for all subjects, therefore age at infusion was imputed based on expected age using the study protocol. This study was approved by the Institutional Review Board and informed consent was obtained from parents/guardians in accordance with federal and institutional guidelines. All procedures performed in studies involving human participants were in accordance with the ethical standards of the 1964 Helsinki declaration [28].

### 2.2 Drug Administration and Supportive Care

All patients enrolled received the same chemotherapy regimen, an intensified induction including high-dose methotrexate, and supportive care as described previously [28]. Subjects received their first cycle of methotrexate at week

4 of induction/intensification. High-dose methotrexate was administered as a 24 h intravenous infusion, with a 200 mg/m<sup>2</sup> loading dose over 20 min, followed by a 3.8 g/m<sup>2</sup> dose over the remainder of the 24 h. This dosing regimen was repeated at week 5 of induction intensification and in consolidation at weeks 11 and 12 of therapy. Standard supportive care for high-dose methotrexate was provided, including hydration with alkalized intravenous fluids and leucovorin rescue. Methotrexate plasma concentrations are reported here as micromoles/L (μM) [28].

### 2.3 Pharmacokinetic (PK) Sampling

Beginning with the first cycle of methotrexate administered at week 4, standard methotrexate monitoring was performed for all subjects at the end of drug infusion and 24 h later. Subsequent concentrations were monitored every 12–24 h until the methotrexate concentration was < 0.18 μM. This standard monitoring was also performed during weeks 5, 11, and 12 of therapy. In addition to this, subjects enrolled in the PK substudy had intensive methotrexate PK sampling at 1, 6, 12, and 23 h after the start of methotrexate infusions [28].

### 2.4 Bioanalytical Assay

Samples obtained as part of standard methotrexate monitoring were analyzed in the clinical laboratories of the treating hospitals. The most common assays used for quantification of methotrexate included fluorescence polarization immunoassay and the enzyme-multiplied immunoassay [29, 30]. For the PK substudy, samples were analyzed at the central study laboratory at Texas Children's Hospital using a high-performance liquid chromatography (HPLC) method [31]. For all methotrexate samples included in this analysis, a conservative lower limit of quantification (LLQ) of 0.05 μM was assumed, which is used commonly in clinical practice [14, 28].

### 2.5 Population PK Model Development

Population PK analyses were performed with NONMEM<sup>®</sup> version 7.4 (ICON Development Solutions, Ellicott City, MD, USA) using methotrexate concentration versus time data for all infants with methotrexate concentration data. The effect of log-transforming methotrexate concentration data was investigated. The first-order conditional estimation (FOCE) method with interaction was applied for all model runs. All data manipulation and visualization of diagnostic plots were executed using R version 3.0.2 (R Foundation for Statistical Computing, Vienna, Austria), and RStudio version 0.99 (RStudio, Boston, MA, USA), with the packages lattice, latticeExtra, and ggplot2 [32–34]. Model development was guided by run minimization, successful

covariance steps, objective function value (OFV) changes for each nested model, plausibility and precision of parameter estimates, evaluation of eta and epsilon shrinkage, reduction in residual variability, and manual inspection of diagnostic plots including visual prediction checks (VPCs).

Both one- and two-compartment structural models were evaluated. The base model assumed a standard allometric scale based on total body weight (WT). A single exponential value of 0.75 was assumed for clearance (CL) and intercompartmental CL (Q), and a single exponential value of 1.0 was assumed for central volume of distribution (V<sub>c</sub>) and peripheral volume of distribution (V<sub>p</sub>) [17, 35]. Estimation of these exponents was also investigated. Standard PK equations were applied for a two-compartment model using the ADVAN3 TRANS4 subroutines in NONMEM<sup>®</sup>. Inter-individual variability (IIV) was assessed for all PK model parameters using an exponential relationship as shown below for a two-compartment model (Eqs. 1–4).

$$CL_i = \theta_{CL, std} \times \left( \frac{WT_i}{70 \text{ kg}} \right)^{0.75} \times \exp(\eta_{i, CL}), \quad (1)$$

$$V_{c, i} = \theta_{V_c, std} \times \left( \frac{WT_i}{70 \text{ kg}} \right)^{1.0} \times \exp(\eta_{i, V_c}), \quad (2)$$

$$V_{p, i} = \theta_{V_p, std} \times \left( \frac{WT_i}{70 \text{ kg}} \right)^{1.0} \times \exp(\eta_{i, V_p}), \quad (3)$$

$$Q_i = \theta_{Q, std} \times \left( \frac{WT_i}{70 \text{ kg}} \right)^{0.75} \times \exp(\eta_{i, Q}), \quad (4)$$

where CL<sub>*i*</sub>, V<sub>*c,i*</sub>, V<sub>*p,i*</sub>, and Q<sub>*i*</sub> are the individual values of CL, V<sub>c</sub>, V<sub>p</sub> and Q, respectively; θ<sub>CL, std</sub>, θ<sub>V<sub>c</sub>, std</sub>, θ<sub>V<sub>p</sub>, std</sub>, and θ<sub>Q, std</sub> are the respective parameter values for a subject with a body weight of 70 kg; WT<sub>*i*</sub> is the individual subject weight; η<sub>*i, CL*</sub>, η<sub>*i, V<sub>c</sub>*</sub>, η<sub>*i, V<sub>p</sub>*</sub>, and η<sub>*i, Q*</sub> are random effect parameters assumed to be symmetrically distributed with a mean equal to zero and variance estimated as ω<sub>CL</sub><sup>2</sup>, ω<sub>V<sub>c</sub></sub><sup>2</sup>, ω<sub>V<sub>p</sub></sub><sup>2</sup> and ω<sub>Q</sub><sup>2</sup>, which describe each individual's variation from the population estimate. Covariance between these variability estimates was evaluated for each parameter. In addition to the IIV, IOV was also characterized for each PK parameters as follows (Eq. 5):

$$\text{Parameter value}_{i, k} = \text{typical value} \times \exp(\eta_i + \kappa_i), \quad (5)$$

where *i* indicates the *i*th individual, *k* indicates the *k*th occasion, the typical value is the mean value of the parameter in the population, η<sub>*i*</sub> is the random effect accounting for IIV, and κ<sub>*i*</sub> is the random effect accounting for IOV [36, 37].

Each treatment cycle was treated as a different occasion, and IOV was assumed to be the same across occasions. Both additive, exponential, and combined residual error models were tested.

Covariates available for analysis included weight, age, body surface area (BSA), and sex. Covariates were evaluated for the model in a stepwise fashion based on changes in the OFV, first by forward inclusion ( $p < 0.05$  and  $\Delta\text{OFV} > 3.8$ ), followed by backward elimination ( $p < 0.001$  and  $\Delta\text{OFV} > 10.8$ ). Both continuous and categorical covariates were tested using the power model normalized as follows (Eqs. 6 and 7):

$$P_{i,j} = \theta_{\text{pop, std}} \times \left( \frac{\text{cov}_i}{\text{cov}_m} \right)^{\theta_{\text{cov}}}, \quad (6)$$

$$P_{i,j} = \theta_{\text{pop, std}} \times \theta_{\text{cov}}^{\text{CATEGORICAL}}, \quad (7)$$

where  $P_{i,j}$  indicates the  $j$ th parameter estimate of the  $i$ th individual,  $\theta_{\text{pop, std}}$  indicates the population parameter values for a subject with a body weight of 70 kg,  $\text{cov}_i$  indicates

the individual covariate value for the  $i$ th individual,  $\text{cov}_m$  indicates the median population covariate value,  $\theta_{\text{cov}}$  is the parameter indicating the covariate effect, and CATEGORICAL is a categorical variable that can take on values of zero or one.

## 2.6 Model Evaluation

The precision of the final population PK model parameter estimates were evaluated using non-parametric bootstraps with 1000 replicates to generate 95% confidence intervals of each parameter using the percentile method [38]. VPCs were run on key models to assess model performance and robustness. VPCs were performed using Perl-speaks-NONMEM (version 3.6.2) and visualized in R using xpose4 [39, 40].

## 2.7 Model Simulations

For all simulations, a virtual population of 1000 infants was created, assuming all subjects were of full gestational age and had a similar weight distribution as our study

**Fig. 1** Methotrexate plasma concentrations from 229 cycles in 71 infants subset by treatment cycle. The  $x$  axis represents the time after the start of the 24 h methotrexate infusion, and the  $y$  axis represents plasma methotrexate on a log scale

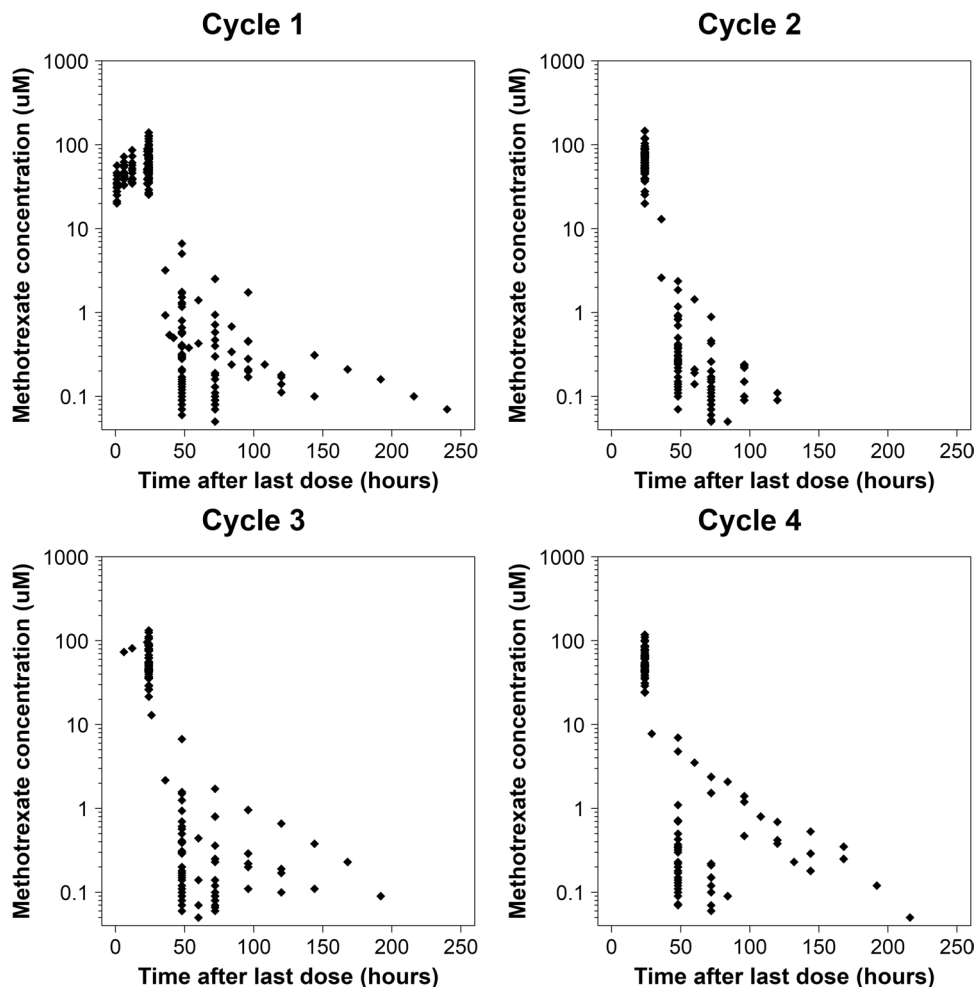


**Table 1** Demographic and clinical characteristics of infants included in the study

Study	Pharmacokinetic substudy group <sup>a</sup> (n = 17)		Routine clinical care group <sup>b</sup> (n = 54)	
	Median	Range	Median	Range
Postnatal age (months) <sup>c</sup>	8.5	2.9–12.9	7.0	1.0–12.9
Total body weight (kg) <sup>c</sup>	8.6	4.5–11.9	7.6	3.0–12.1
Height (cm) <sup>c</sup>	69	51–78	66.5	49.7–79.0
Body surface area (m <sup>2</sup> ) <sup>c</sup>	0.40	0.24–0.48	0.36	0.20–0.48
Methotrexate dose (g)	1.5	0.62–1.96	1.4	0.60–2.2
Methotrexate dose (g/m <sup>2</sup> )	4.0	2.0–4.5	4.0	2.0–5.6
Methotrexate C <sub>24h</sub> (μM)	54.7	24.2–146.6	61.5	24.0–140.0
Methotrexate C <sub>48h</sub> (μM)	0.20	0.07–7.0	0.20	0.06–6.7
Methotrexate C <sub>72h</sub> (μM)	0.17	0.07–2.4	0.11	0.05–2.5

*Methotrexate dose* total dose administered as a 24-h infusion, *C<sub>xh</sub>* plasma concentration of methotrexate at x hours

<sup>a</sup>8 males, 9 females

<sup>b</sup>24 males, 30 females

<sup>c</sup>Reported at first treatment course

population. Monte Carlo simulations were performed to assess the frequency of subtherapeutic and suprathreshold methotrexate concentrations with doses of 2, 4, 6, and 8 g/m<sup>2</sup> of methotrexate administered intravenously over 24 h. For each dose, methotrexate concentrations were simulated at 2, 6, 8, 24, 42, 48, 72, 96, 120, 144, 168, 216, and 240 h. Simulations were repeated to generate four cycles of simulated methotrexate concentrations for each subject. Target methotrexate concentrations were defined based on previous literature suggesting that methotrexate concentrations < 16 μM at 24 h are associated with relapse and are subtherapeutic, and methotrexate concentrations > 100 μM at 24 h, > 1.0 μM at 48 h, and > 0.1 μM at 72 h are associated with increased toxicity and are suprathreshold [41, 42].

The R package mlxR was used to simulate a ‘bedside algorithm’ for individualizing high-dose methotrexate exposure similar to that proposed previously [43, 44]. This algorithm adjusts the rate of methotrexate infusion according to methotrexate concentrations obtained at 2 and 6 h after the start of a 24 h intravenous infusion of methotrexate 4 g/m<sup>2</sup>. Simulations maintained an infusion length of 24 h, which is known to be essential to the antitumor activity of methotrexate. At 2 h, the infusion rate was decreased by 50% in subjects with methotrexate concentrations > 100 μM. At 6 h, the infusion rate was decreased by 25% for subjects with methotrexate concentrations between 75 and 100 μM, and the

infusion rate was decreased by 50% in subjects with methotrexate concentrations > 100 μM. The percentage of subjects requiring dose adjustment was calculated, and the median 24 h methotrexate concentration was compared between subjects who did or did not require dose adjustments.

## 3 Results

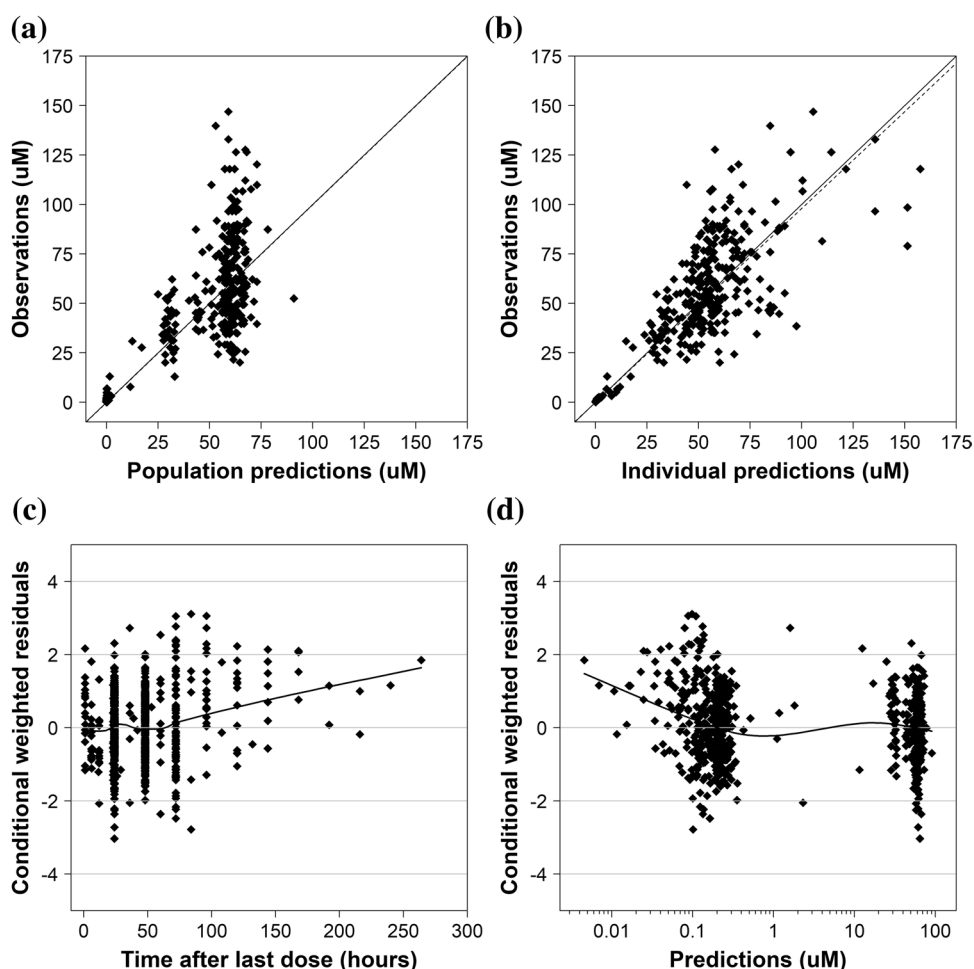
### 3.1 Patient Data

A total of 690 methotrexate concentrations were available from 71 subjects who underwent 229 cycles of high-dose methotrexate treatment of ALL. There were 2.6% (18/690) methotrexate concentrations below the LLQ of 0.05 μM, all of which were excluded [45]. The PK profile of all 71 subjects stratified by cycle is shown in Fig. 1. Intensive methotrexate PK sampling was performed in 24.0% (17/71) of subjects enrolled, and 92.0% (65/71) of subjects had PK data for more than one occasion. Of subjects who had intensive PK monitoring, 94.1% (16/17) of these intensive collections occurred during cycle 1. There were no differences in the baseline demographics between subjects in the PK substudy and the routine clinical care group (Table 1). For the majority of methotrexate cycles, subjects received methotrexate doses close to 4 g/m<sup>2</sup>. However, for 14.4% (33/229) of cycles, patients received doses < 3.5 g/m<sup>2</sup> (median 2.99 g/m<sup>2</sup>, range 2.0–3.48), and, for 1.3% (3/229) of cycles, subjects received doses > 4.5 g/m<sup>2</sup> (median 5.63 g/m<sup>2</sup>, range 5.34–5.63). The reason for dose modification in these subjects is unknown to us.

### 3.2 Population PK Analysis

Methotrexate plasma concentrations were best characterized by a two-compartment model with linear elimination. Data was log-transformed as model minimization was not achievable using raw concentrations, likely due to the wide range of concentrations. After allometrically scaled total body weight was incorporated into CL, *V<sub>c</sub>*, *V<sub>p</sub>*, and *Q* terms, no other covariates were found to be significant. Visual inspection of the eta plots revealed a weak association between age and CL, but incorporating this as a covariate reduced the OFV by < 3.8. Visual inspection of the empirical Bayesian estimates (EBEs) of CL did not reveal a correlation with age or treatment cycle (electronic supplemental material). Estimation of the allometric scaling factors for CL and volume of distribution terms did not improve the OFV, but increased the shrinkage of IIV estimates and resulted in estimates similar to fixed exponents, i.e. 0.80 and 0.98, respectively, and these were therefore fixed. The final model included estimation of the IIV on both CL and *V<sub>c</sub>*, as well as IOV

**Fig. 2** Diagnostic plots of the final population pharmacokinetic model. **a** Population-predicted concentrations versus observations; **b** individual predictions versus observations; **c** time after last dose versus conditional weighted residuals; and **d** population-predicted concentrations versus conditional weighted residuals. For **a** and **b**, the dashed line represents the line of unity and the solid line represents a linear regression. For **c** and **d**, the black line represents the LOESS curve, and the gray lines represent conditional weighted residual values of  $-4$ ,  $-2$ ,  $0$ ,  $2$ , and  $4$ . LOESS locally weighted scatterplot smoothing



on CL. A correlation between the IIV of CL and  $V_c$  was noted in diagnostic plots, however this was not included in the final model as estimation of this term resulted in a relatively small correlation coefficient (0.383) and did not allow for a successful covariance step. Estimation of IIV and IOV on other model parameters was not included in the final model due to inflation of the eta shrinkage values to  $> 60\%$  for IIV estimates. The final model included a single proportional residual error model for all methotrexate concentrations.

The diagnostic plots for the final population PK model are shown in Fig. 2. These plots demonstrate some misspecification in the population predictions, which is improved with the incorporation of IIV and IOV in the individual predictions. Additionally, while panel C appears to show misspecification occurring at concentrations observed at  $> 200$  h after dosing, this is likely due to the small number of methotrexate observations. The final model PK parameters, standard errors, and results of the bootstrap analysis are shown in Table 2. Overall, there was a relatively high degree of IOV on CL (25.4%) compared with both the IIV on CL (10.7%) and IIV on  $V_c$  (13.2%). All parameter estimates fell within

10% of the median bootstrap estimates, suggesting reasonable precision of parameter estimates. Four example subjects who demonstrated a high degree of IOV in their methotrexate CL are shown in Fig. 3. The results of the VPC are shown in Fig. 4, and demonstrate that the model captures the observed variability well. Notably, 11.9% (80/672) of the observations fell outside of the 90% prediction interval, suggesting a slight underestimation of the random effects. Few methotrexate observed concentrations fell below the 5% prediction interval, suggesting the final model prediction for CL may be slightly overestimated. These results were similar when a VPC was performed focusing solely on the first 72 h after infusion (electronic supplementary material).

### 3.3 Model Simulations

The results of the dose-ranging simulation are shown in Table 3. None of the dosing regimens evaluated resulted in simulated 24 h methotrexate concentrations  $< 16 \mu\text{M}$ . Additionally, compared with the study dose of  $4 \text{ g/m}^2$ , escalating doses of 6 and  $8 \text{ g/m}^2$  resulted in a substantial increase in the percentage of simulated supratherapeutic methotrexate

**Table 2** Final population pharmacokinetic model parameter estimates and bootstrap results

Parameter	Final model Estimate (RSE%) <sup>b</sup>	Bootstrap analysis [ <i>N</i> = 1000] <sup>a</sup>		
		5th percentile	Median	95th percentile
Fixed effects <sup>c</sup>				
$\theta_{CL, std}$ (L/h/70 kg)	11.0 (3.1)	10.4	11.0	11.6
$\theta_{V_c, std}$ (L/70 kg)	63.4 (5.1)	57.2	62.9	69.0
$\theta_{V_p, std}$ (L/70 kg)	13.6 (8.5)	10.6	13.3	15.6
$\theta_{Q, std}$ (L/h/70 kg)	0.13 (7.6)	0.11	0.13	0.15
IIV <sup>d</sup>				
$\omega_{CL}$ (IIV as CV%)	10.7 (49.7)	5.23	10.7	14.7
$\omega_{V_c}$ (IIV as CV%)	13.2 (56.2)	5.74	12.7	18.7
IOV <sup>e</sup>				
$\omega_{CL, IOV}$ (IOV as CV%)	25.4 (21.1)	20.9	25.3	29.8
Residual variability <sup>e</sup>				
Proportional error (%)	37.5 (7.52)	34.9	37.2	39.6

IIV interindividual variability, CV% percentage coefficient of variation, IOV interoccasion variability

<sup>a</sup>A total of 951 runs (95.1%) successfully minimized and 1000 (100%) runs completed the covariance step

<sup>b</sup>RSE is the relative standard error defined as the standard error of the estimate divided by the final parameter estimate multiplied by 100

<sup>c</sup>Theory-based allometry was applied such that model parameters are standardized to a 70 kg adult, assuming an exponent of 0.75 for clearance terms and 1.0 for volume of distribution terms;  $\theta_{CL, std}$  is the population clearance standardized to a 70 kg adult,  $\theta_{V_c, std}$  is the population central volume of distribution standardized to a 70 kg adult,  $\theta_{V_p, std}$  is the population peripheral volume of distribution standardized to a 70 kg adult, and  $\theta_{Q, std}$  is the population intercompartmental clearance standardized to a 70 kg adult

<sup>d</sup>Model estimates reported in CV%;  $\omega_{CL}$  is the variance of the IIV for clearance,  $\omega_{V_c}$  is the variance of the IIV for volume, and  $\omega_{CL, IOV}$  is the variance of the IOV on clearance

<sup>e</sup>Proportional residual error coded as additive on logarithmic scale

concentrations. The percentage of subjects with supratherapeutic methotrexate concentrations at 72 h (> 0.1  $\mu\text{M}$ ) was high for all simulated doses, similar to the exposures in our subjects who received 4  $\text{g}/\text{m}^2$ . This suggests further research may be needed to define supratherapeutic concentrations at 72 h in this patient population.

Simulation of a bedside algorithm showed that without dose adjustment, 21.1% (211/1000) of infants receiving a single cycle of 4  $\text{g}/\text{m}^2$  would be expected to achieve supratherapeutic methotrexate concentrations, similar to published reports [43, 46]. A total of 214 dose adjustments were made, of which 1.87% (4/214) were a 50% decrease in infusion rate at 2 h due to a simulated methotrexate concentration > 100  $\mu\text{M}$ , 29.0% (62/214) were a 50% decrease in infusion rate at 6 h due to a simulated methotrexate concentration > 100  $\mu\text{M}$ , and 69.2% (148/214) were a 25% decrease in infusion rate at 6 h due to a simulated methotrexate concentration between 75 and 100  $\mu\text{M}$ . All four simulated infants who required dose adjustment at 2 h also required adjustment at 6 h, and therefore 21.1% (211/1000) of simulated infants had their dose modified by the algorithm. As shown in Fig. 5, dose adjustment using this bedside algorithm resulted in similar median (25th percentile–75th percentile) 24 h methotrexate concentrations between subjects requiring dose adjustment and those who did not, i.e. 58.8  $\mu\text{M}$

(50.5–69.2) and 59.1  $\mu\text{M}$  (49.5–69.7), respectively. These results suggest that the application of a simple algorithm to adjust the methotrexate infusion rate may make targeted methotrexate exposure more feasible, and can overcome the challenge of IOV in methotrexate CL between cycles.

## 4 Discussion

TDM of high-dose methotrexate remains an essential practice for identifying subjects at risk for methotrexate toxicity and informing supportive care measures [14, 47]. Previous research has shown that individualization of methotrexate exposure using TDM can reduce the incidence of methotrexate toxicity and improve patient outcomes [41, 46]. Individualization of methotrexate exposure is challenging due to the known within-subject and between-subject variability of methotrexate CL, which may be better characterized using population PK modeling [24, 48, 49]. Therefore, the objective of our study was to develop a population PK model of methotrexate in infants with ALL, and to quantify the effects of IOV between cycles on this PK model.

To date, this is the largest population PK model of high-dose methotrexate in infant ALL, and the first to include infants as young as 2 months PNA. Our PK dataset consisted

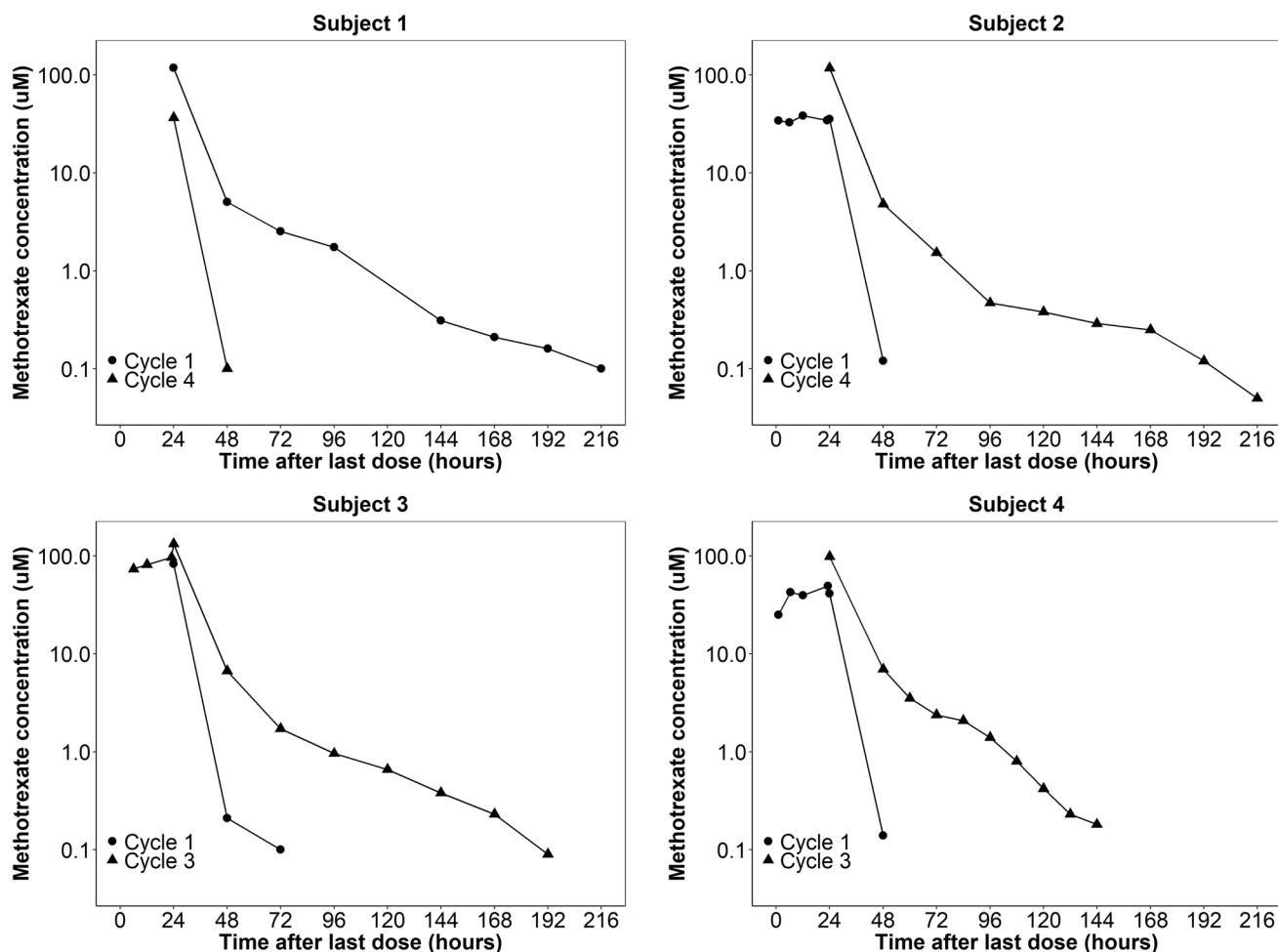


**Fig. 3** Four infants demonstrating high interoccasion variability in their clearance of methotrexate. Each subject received the same weight-based dose of high-dose methotrexate  $4 \text{ g/m}^2$ . The  $x$  axis represents

the time after the start of the 24 h methotrexate infusion, and the  $y$  axis represents plasma methotrexate concentrations on log scale

of methotrexate plasma concentrations collected as part of routine care, combined with methotrexate plasma concentrations from infants enrolled in a PK substudy [28]. The PK substudy data significantly improved model fitting by increasing the total number of methotrexate concentrations and by providing methotrexate concentration data, drawn during the infusion, that were informative for methotrexate parameter estimation. Additionally, our PK dataset contained multiple cycles of methotrexate concentrations, which allowed us to quantify the within-subject variability in PK parameters, across cycles, as IOV.

A two-compartment model best characterized the PK of methotrexate in the 71 infants in our study, which is consistent with previous reports of high-dose methotrexate in both children and adults [46, 48, 50–57]. Our model applied theory-based allometry to scale CL and volume of distribution parameters to a standard weight of 70 kg [17, 58]. The resulting final model CL and  $V_c$  estimates scaled to a 70 kg adult are similar to published reports in adults [52, 59, 60].

Additionally, a retrospective case–control study comparing the PK of high-dose methotrexate in pediatric ALL subjects applied an identical methodology for allometric scaling of CL and  $V_d$  terms [51]. The final parameter estimates scaled to a 70 kg adult from this previously published model were a CL of  $13 \text{ L/h/70 kg}$  and a  $V_c$  of  $46 \text{ L/70 kg}$ , which compare favorably with our estimates of  $11.0 \text{ L/h/70 kg}$  and  $63.4 \text{ L/70 kg}$ , respectively. Our weight-normalized final model estimate of CL was  $0.273 \text{ L/h/kg}$ , which falls within the range of reported adult and pediatric literature values of  $0.117\text{--}0.374 \text{ L/h/kg}$ . Similar to our estimate for CL, our final model estimate of  $V_c$  of  $0.910 \text{ L/kg}$  falls within the range of reported values of  $0.356\text{--}1.27 \text{ L/kg}$  in adult and pediatric subjects [30, 48, 50, 55–57, 61].

We did not identify age as a covariate impacting CL, which has been described previously [46, 48, 62–64]. However, the impact of age on methotrexate CL has been reported inconsistently as there are multiple published PK analyses that have found no impact of age on the CL of



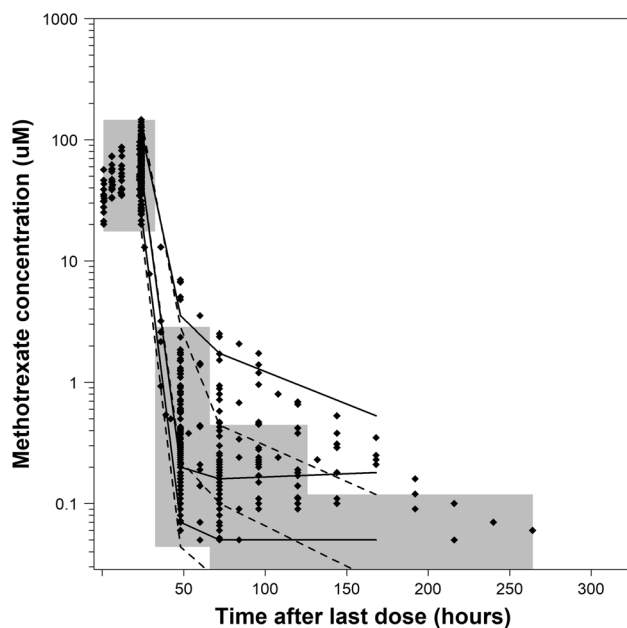


**Fig. 4** Final model visual predictive check. A total of 80 points (11.9%) fell outside the 90% prediction interval. Dotted and solid lines represent the 5th, 50th, and 95th percentiles of the simulated data and observed data, respectively, and gray-shaded areas represent the 90% prediction interval. The  $x$  axis represents the time after the start of the 24 h methotrexate infusion, and the  $y$  axis represents plasma methotrexate concentrations on log scale

methotrexate in pediatric subjects [50, 54, 57]. The effect of renal maturation, reflected by modeling PNA as a covariate on methotrexate CL, would be expected to be highest in both premature infants as well as full-term infants < 6 months of age [17–20]. Therefore, it is possible that we were unable to identify PNA as a significant covariate on methotrexate CL because our data only included 28.4% (65/229) of cycles

with infants < 6 months of age, and premature infants were subsequently excluded from this study.

Our study demonstrated a similar magnitude of IOV in the CL of methotrexate compared with previous studies performed in children [48, 51, 65]. This variation in the CL of methotrexate across cycles may be explained by changes in disease progression, drug–drug interactions, or unmeasured covariates that vary across cycles. The magnitude of IOV in the CL of methotrexate suggests that Bayesian adaptive dosing algorithms may be optimized by obtaining methotrexate concentrations during the current cycle infusion, rather than concentrations measured from previous cycles.

Simulations revealed that dosing regimens of 2–8 g/m<sup>2</sup> provide sufficient methotrexate exposure based on the 24 h methotrexate target of 16 µM [41]. However, increasing doses of high-dose methotrexate above 4 g/m<sup>2</sup> may result in untoward renal toxicity as > 15% of all simulated infants would have experienced supratherapeutic methotrexate concentrations. Application of the final population PK model using a bedside dosing algorithm revealed the potential clinical impact of our protocol as our simulated individualization strategy reduced supratherapeutic methotrexate concentrations in 21.1% of simulated subjects. Future prospective studies individualizing methotrexate exposure using a similar approach are needed to evaluate the impact of such a bedside algorithm on patient outcomes.

Our study has several limitations. First, it included limited covariates, and notably we did not have markers of renal function. Despite this, all infants were screened for adequate organ function prior to each methotrexate treatment cycle, including a creatinine CL > 70 mL/min/1.73 m<sup>2</sup>. Therefore it is unlikely markers for renal function would have improved model fitting [48, 66]. Other missing potential covariates included serum albumin, urine pH, pharmacogenomic data,

**Table 3** Simulation results of 1000 virtual patients treated with four cycles of high-dose methotrexate

Clinical endpoint	Dose of methotrexate simulated (g/m <sup>2</sup> )			
	2	4	6	8
MTX C <sub>24h</sub> (µM) <sup>a</sup>	33.5 (27.9–40.0)	67.4 (55.7–79.8)	100.5 (83.7–119)	134.3 (111–159)
MTX C <sub>48h</sub> (µM) <sup>a</sup>	0.125 (0.0735–0.235)	0.250 (0.147–0.470)	0.375 (0.221–0.705)	0.501 (0.295–0.940)
MTX C <sub>72h</sub> (µM) <sup>a</sup>	0.0672 (0.0592–0.0983)	0.134 (0.0907–0.196)	0.202 (0.135–0.292)	0.267 (0.181–0.392)
Subtherapeutic at 24 h <sup>b</sup> (%)	0	0	0	0
Supratherapeutic at 24 h <sup>c</sup> (%)	0.3	6.28	51.1	85.5
Supratherapeutic at 48 h <sup>c</sup> (%)	3.05	9.43	16.4	23.3
Supratherapeutic at 72 h <sup>c</sup> (%)	24.0	69.3	89.0	95.6
Time to MTX < 0.05 µM <sup>d</sup>	42 (42–72)	42 (42–48)	42 (42–96)	42 (42–120)

MTX methotrexate

<sup>a</sup>MTX C <sub>$x$</sub>  is the simulated methotrexate concentration at time  $x$  reported as the median (25th–75th percentile)

<sup>b</sup>The percentage of subtherapeutic subjects at 24 h (< 16 µM)

<sup>c</sup>The percentage of supratherapeutic subjects at 24 h (> 100 µM), 48 h (> 1 µM) and 72 h (> 0.1 µM)

<sup>d</sup>Reported in hours as median (minimum–maximum)

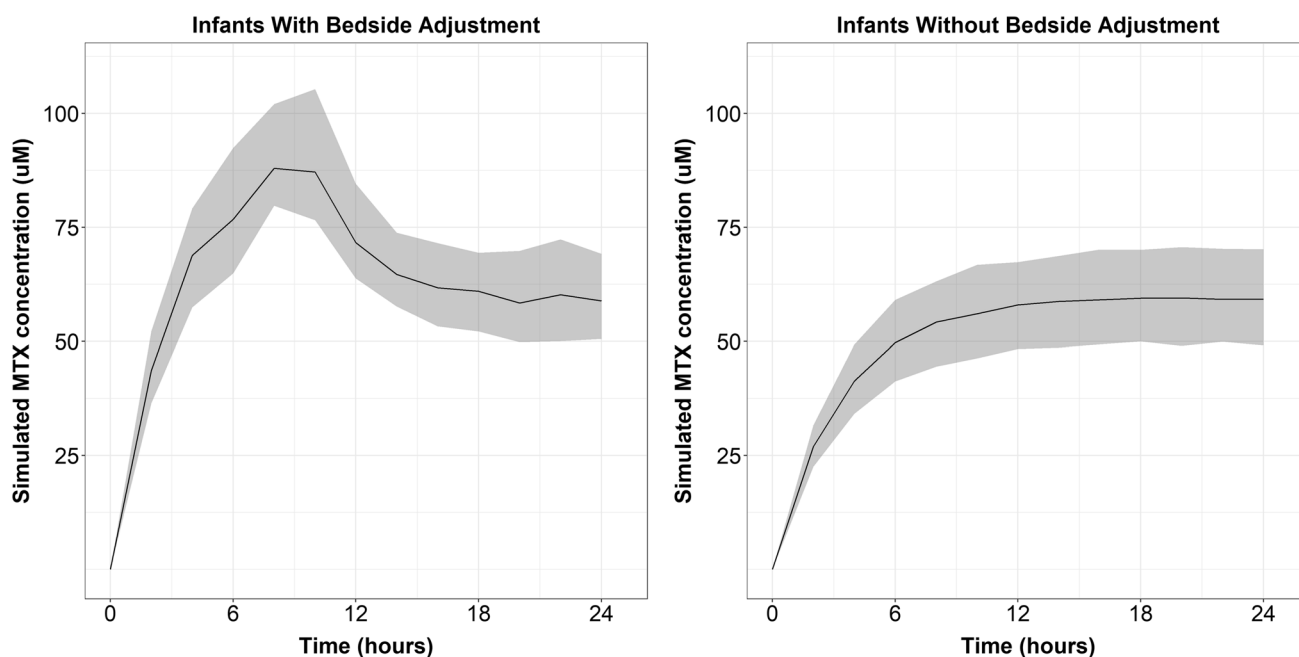


**Fig. 5** Simulated MTX exposures in 1000 virtual infants using a bedside adjustment with the R package *mlxR*. This algorithm adjusts the rate of MTX infusion according to MTX concentrations obtained at 2 and 6 h after the start of a single 24 h intravenous infusion of methotrexate 4 g/m<sup>2</sup>. At 2 h, the infusion rate was decreased by 50% in subjects with MTX concentrations > 100  $\mu$ M. At 6 h, the infusion rate was decreased by 25% for subjects with MTX concentrations between 75 and 100  $\mu$ M, and the infusion rate was decreased by 50%

in subjects with MTX concentrations > 100  $\mu$ M. The x axis represents the time after the start of infusion, and the y axis shows simulated MTX concentrations. The dark black line denotes the median MTX concentration, and the gray-shaded region shows the 25th–75th percentiles of simulated MTX concentrations. The left panel shows simulated MTX concentrations in subjects requiring bedside adjustment (211/1000), and the right panel shows simulated MTX concentrations in subjects without dose adjustment (789/1000). *MTX* methotrexate

and concomitant drug use [67–70]. A second limitation is that the exact age of each infant during methotrexate infusion was not available, and therefore there may have been discrepancies between ages used for modeling and true age during infusion. A third limitation is that the methotrexate concentrations we chose as targets for our simulation have not been prospectively validated. Therefore, future studies are still needed to elucidate the relationship between methotrexate concentrations and both efficacy and toxicity. A fourth limitation of our analysis is that intensive PK sampling was not evenly distributed across treatment cycles, and this may limit our ability to estimate true IOV in methotrexate CL across treatment cycles. Despite these limitations, our results add to the dearth of literature on the PK of methotrexate in infants with ALL, and provide additional evidence of the potential benefit of individualized dosing strategies.

## 5 Conclusion

We characterized the population PK of methotrexate in infants with ALL using a two-compartment model allometrically scaled by body size. Infants treated in our study demonstrated a relatively high degree of IOV in methotrexate

CL across treatment cycles. These analyses suggest that individualization of methotrexate therapy may be improved by performing additional monitoring and dose adjustment during methotrexate infusions to account for the change in methotrexate CL occurring across treatment cycles.

**Acknowledgements** Research reported in this publication was supported by the Children’s Oncology Group Chair’s Grant U10CA098543 and Statistics & Data Center Grant U10CA098413, the National Clinical Trials Network (NCTN) Operations Center Grant U10CA180886, the NCTN Statistics and Data Center Grant U10CA180899, and St. Baldrick’s Foundation. PAT and RCV wish to acknowledge the contributions of Jeff Barrett, Ph.D., Head of Quantitative Sciences at Bill & Melinda Gates Medical Research Institute, and Peter L. Bonate, Ph.D., Global Head, Pharmacokinetics, Modeling, and Simulation, Astellas Pharmaceuticals, for their NONMEM® and PK modeling education.

## Compliance with Ethical Standards

**Conflicts of Interest** Ryan J. Beechinor, Patrick A. Thompson, Ryan C. Vargo, Michael F. Hwang, Lisa R. Bomgaars, Jacqueline G. Gerhart, ZoAnn E. Dreyer, and Daniel Gonzalez declare that they have no conflicts of interest.

**Funding** RJB is supported by the National Institute of General Medical Sciences (NIGMS) of the National Institutes of Health (NIH) under award T32GM086330; MFH is funded by a IQVIA Pharmacometrics

Fellowship; and DG receives support for research from the Eunice Kennedy Shriver National Institute of Child Health and Human Development (K23HD083465). The remaining authors have no relevant funding to disclose. The content is solely the responsibility of the authors and does not represent the official views of the NIH.

**Ethical Approval** All procedures performed in studies involving human participants were in accordance with the ethical standards of the institutional and/or national research committee and with the 1964 Helsinki declaration and its later amendments or comparable ethical standards.

**Informed Consent** Informed consent was obtained from parents/guardians in accordance with federal and institutional guidelines.

## References

- Howlander N, Noone A, Krapcho M, Miller D, Bishop K, Kosary CL, et al. SEER Cancer Statistics Review, 1975–2014. National Cancer Institute. 2016. [https://seer.cancer.gov/csr/1975\\_2014/](https://seer.cancer.gov/csr/1975_2014/). Accessed 24 Apr 2018.
- Terwilliger T, Abdul-Hay M. Acute lymphoblastic leukemia: a comprehensive review and 2017 update. *Blood Cancer J*. 2017;7:e577.
- Inaba H, Greaves M, Mullighan C. Acute lymphoblastic leukemia. *Lancet*. 2013;381:1943–55.
- Pieters R. Infant acute lymphoblastic leukemia: Lessons learned and future directions. *Pediatr Malig Hematol*. 2009;4(3):167–74.
- Hilden JM, Dinndorf PA, Meerbaum SO, Sather H, Villaluna D, Heerema NA, et al. Analysis of prognostic factors of acute lymphoblastic leukemia in infants: report on CCG 1953 from the Children's Oncology Group. *Blood*. 2006;108(2):441–4.
- Palle J, Frost BM, Forestier E, Gustafsson G, Nygren P, Hellebostad M, et al. Cellular drug sensitivity in MLL-rearranged childhood acute leukaemia is correlated to partner genes and cell lineage. *Br J Haematol*. 2005;129(2):189–98.
- Kotecha RS, Gottardo NG, Kees UR, Cole CH. The evolution of clinical trials for infant acute lymphoblastic leukemia. *Blood Cancer J*. 2014;4(4):e200.
- Bleyer WA. Methotrexate: clinical pharmacology, current status and therapeutic guidelines. *Cancer Treat Rev*. 1977;4(2):87–101.
- Bleyer WA. The clinical pharmacology of methotrexate new applications of an old drug. *Cancer*. 1978;41(1):36–51.
- Baram J, Allegra CJ, Fine RL, Chabner BA. Effect of methotrexate on intracellular folate pools in purified myeloid precursor cells from normal human bone marrow. *J Clin Invest*. 1987;79(3):692–7.
- Goldman D, Matherly LH, Goldman ID, Matherly LH. The cellular pharmacology of methotrexate. *Pharmacol Ther*. 1985;28(1):77–102.
- Gökbuget N, Hoelzer D. High-dose methotrexate in the treatment of adult acute lymphoblastic leukemia. *Ann Hematol*. 1996;72(4):194–201.
- Evans WE, Crom WR, Abromowitch M, Dodge R, Look AT, Bowman WP, et al. Clinical pharmacodynamics of high-dose methotrexate in acute lymphocytic leukemia. *N Engl J Med*. 1986;314(8):471–7.
- Howard SC, McCormick J, Pui C-H, Buddington RK, Harvey RD. Preventing and managing toxicities of high-dose Methotrexate. *Oncologist*. 2016;21(12):1471–82.
- Methotrexate injection [prescribing information]. Lake Forest, IL: Hospira Inc; 2014.
- Huffman DH, Wan SH, Azarnoff DL, Hoogstraten B, Hogstraten B. Pharmacokinetics of methotrexate. *Clin Pharmacol Ther*. 1973;14(4):572–9.
- Holford N, Heo Y-AA, Anderson B. A pharmacokinetic standard for babies and adults. *J Pharm Sci*. 2013;102(9):2941–52.
- Siegel SE, Moran RG. Problems in the chemotherapy of cancer in the neonate. *Am J Pediatr Hematol Oncol*. 1981;3(3):287–96.
- Mihsap RL, Jusko WJ. Pharmacokinetics in the infant. *Env Heal Perspec*. 1994;102(Suppl 11):107–10.
- Stewart C, Hampton E. Effect of maturation on drug disposition in pediatric patients. *Clin Pharm*. 1987;6(7):548–64.
- McLeod HL, Relling MV, Crom WR, Silverstein K, Groom S, Rodman JH, et al. Disposition of antineoplastic agents in the very young child. *Br J Cancer*. 1992;18:S23–9.
- Friis-Hansen BJ, Holiday M, Stapleton T, Wallace WM. Total body water in children. *Pediatrics*. 1951;7(3):321–7.
- Lönnerholm G, Valsecchi MG, De Lorenzo P, Schrappe M, Hovi L, Campbell M, et al. Pharmacokinetics of high-dose methotrexate in infants treated for acute lymphoblastic leukemia. *Pediatr Blood Cancer*. 2009;52(5):596–601.
- Donelli MG, Zucchetti M, Robatto A, Perlangeli V, D'Incalci M, Masera G, et al. Pharmacokinetics of HD-MTX in infants, children, and adolescents with non-B acute lymphoblastic leukemia. *Med Pediatr Oncol*. 1995;24(3):154–9.
- Mould DR, Upton RN. Basic concepts in population modeling, simulation, and model-based drug development—part 2: introduction to pharmacokinetic modeling methods. *CPT Pharmacometrics Syst Pharmacol*. 2013;2(4):e38.
- US Food and Drug Administration. Guidance for Industry Population Pharmacokinetics. 1999. <http://www.fda.gov/downloads/Drugs/GuidanceComplianceRegulatoryInformation/Guidances/UCM072137.pdf>. Accessed 24 Apr 2018.
- Joerger M. Covariate pharmacokinetic model building in oncology and its potential clinical relevance. *AAPS J*. 2012;14(1):119–32.
- Thompson PA, Murry DJ, Rosner GL, Lunagomez S, Blaney SM, Berg SL, et al. Methotrexate pharmacokinetics in infants with acute lymphoblastic leukemia. *Cancer Chemother Pharmacol*. 2007;59(6):847–53.
- Fotoohi K, Skärby T, Söderhäll S, Peterson C, Albertioni F. Interference of 7-hydroxymethotrexate with the determination of methotrexate in plasma samples from children with acute lymphoblastic leukemia employing routine clinical assays. *J Chromatogr B*. 2005;817(2):139–44.
- Skärby T, Jönsson P, Hjorth L, Behrentz M, Böjrk O, Forestier E, et al. High-dose methotrexate: on the relationship of methotrexate elimination time vs renal function and serum methotrexate levels in 1164 courses in 264 Swedish children with acute lymphoblastic leukaemia (ALL). *Cancer Chemother Pharmacol*. 2003;51(4):311–20.
- Belz S, Frickel C, Wolfrom C, Nau H, Henze G. High-performance liquid chromatographic determination of methotrexate, 7-hydroxymethotrexate, 5-methyltetrahydrofolic acid, and folinic acid in serum and cerebrospinal fluid. *J Chromatogr B*. 1994;661(1):109–18.
- Sarkar D. Lattice: multivariate data visualization with R. New York: Springer; 2008.
- Sarkar D, Andrews F. latticeExtra: extra graphical utilities based on lattice. 2018. <https://cran.rproject.org/package=latticeExtra>. Published 2016. Accessed 24 Apr 2018.
- Wickham H. Ggplot2: elegant graphics for data analysis. New York: Springer; 2009.
- Anderson BJ, Holford NHG. Mechanistic basis of using body size and maturation to predict clearance in humans. *Drug Metab Pharmacokinet*. 2009;24(1):25–36.
- Karlsson MO, Sheiner LB. The importance of modeling interoccasion variability in population pharmacokinetic analyses. *J Pharmacokinet Biopharm*. 1993;21(6):735–50.

37. Kristoffersson AN, Friberg LE, Nyberg J. Inter occasion variability in individual optimal design. *J Pharmacokinet Pharmacodyn*. 2015;42(6):735–50.
38. Baverel PG, Savic RM, Karlsson MO. Two bootstrapping routines for obtaining imprecision estimates for nonparametric parameter distributions in nonlinear mixed effects models. *J Pharmacokinet Pharmacodyn*. 2011;38(1):63–82.
39. Lindbom L, Pihlgren P, Jonsson EN, Jonsson N. PsN-Toolkit—a collection of computer intensive statistical methods for non-linear mixed effect modeling using NONMEM. *Comput Methods Programs Biomed*. 2005;79(3):241–57.
40. Jonsson EN, Karlsson MO. Xpose: an S-PLUS based population pharmacokinetic/pharmacodynamic model building aid for NONMEM. *Comput Methods Programs Biomed*. 1999;58(1):51–64.
41. Evans WE, Relling MV, Rodman JH, Crom WR, Boyett JM, Pui C-H. Conventional compared with individualized chemotherapy for childhood acute lymphoblastic leukemia. *N Engl J Med*. 1998;338(8):499–505.
42. Widemann BC, Adamson PC. Understanding and managing methotrexate nephrotoxicity. *Oncologist*. 2006;11(6):694–703.
43. Foster JH, Bernhardt MB, Thompson PA, Smith EO, Schafer ES. Using a bedside algorithm to individually dose high-dose methotrexate for patients at risk for toxicity. *J Pediatr Hematol Oncol*. 2017;39(1):72–6.
44. Lavielle M. mlxR: simulation of longitudinal data. R package version 3.3.0. 2018. <https://cran.r-project.org/package=mlxR>. Accessed 24 Apr 2018.
45. Keizer RJ, Jansen RS, Rosing H, Thijssen B, Beijnen JH, Schellens JHM, et al. Incorporation of concentration data below the limit of quantification in population pharmacokinetic analyses. *Pharmacol Res Perspect*. 2015;3(2):e00131.
46. Wall AM, Gajjar A, Link A, Mahmoud H, Pui CH, Relling MV. Individualized methotrexate dosing in children with relapsed acute lymphoblastic leukemia. *Leukemia*. 2000;14(2):221–5.
47. Paci A, Veal G, Bardin C, Levêque D, Widmer N, Beijnen J, et al. Review of therapeutic drug monitoring of anticancer drugs part 1: cytotoxics. *Eur J Cancer*. 2014;50(12):2010–9.
48. Aumente D, Buelga DS, Lukas JC, Gomez P, Torres A, García MJ. Population pharmacokinetics of high-dose methotrexate in children with acute lymphoblastic leukaemia. *Clin Pharmacokinet*. 2006;45(12):1227–38.
49. Lucchesi M, Guidi M, Fonte C, Farina S, Fiorini P, Favre C, et al. Pharmacokinetics of high-dose methotrexate in infants aged less than 12 months treated for aggressive brain tumors. *Cancer Chemother Pharmacol*. 2016;77(4):857–64.
50. Piard C, Bressolle F, Fakhoury M, Zhang D, Yacouben K, Rietord A, et al. A limited sampling strategy to estimate individual pharmacokinetic parameters of methotrexate in children with acute lymphoblastic leukemia. *Cancer Chemother Pharmacol*. 2007;60(4):609–20.
51. Buitenkamp TD, Mathôt RAA, de Haas V, Pieters R, Zwaan CM. Methotrexate-induced side effects are not due to differences in pharmacokinetics in children with Down syndrome and acute lymphoblastic leukemia. *Haematologica*. 2010;95(7):1106–13.
52. Min Y, Qiang F, Peng L, Zhu Z. High dose methotrexate population pharmacokinetics and Bayesian estimation in patients with lymphoid malignancy. *Biopharm Drug Dispos*. 2009;30(8):437–47.
53. Watanabe M, Fukuoka N, Takeuchi T, Yamuguchi K, Motoki T, Tanaka H, et al. Developing population pharmacokinetic parameters for high-dose methotrexate therapy: implication of correlations among developed parameters for individual parameter estimation using the bayesian least-squares method. *Biol Pharm Bull*. 2014;37(6):916–21.
54. Jönsson P, Skärby T, Heldrup J, Schröder H, Höglund P. High dose methotrexate treatment in children with acute lymphoblastic leukaemia may be optimised by a weight-based dose calculation. *Pediatr Blood Cancer*. 2011;57(1):41–6.
55. Dombrowsky E, Jayaraman B, Narayan M, Barrett JS. Evaluating performance of a decision support system to improve methotrexate pharmacotherapy in children and young adults with cancer. *Ther Drug Monit*. 2011;33(1):99–107.
56. Fukuhara K, Ikawa K, Morikawa N, Kumagai K. Population pharmacokinetics of high-dose methotrexate in Japanese adult patients with malignancies: a concurrent analysis of the serum and urine concentration data. *J Clin Pharm Ther*. 2008;33(6):677–84.
57. Rousseau A, Sabot C, Delepine N, Delepine G, Debord J, Lachâtre G, et al. Bayesian estimation of methotrexate pharmacokinetic parameters and area under the curve in children and young adults with localised osteosarcoma. *Clin Pharmacokinet*. 2002;41(13):1095–104.
58. Anderson B, Holford N. Mechanism-based concepts of size and maturity in pharmacokinetics. *Annu Rev Pharmacol Toxicol*. 2008;48:303–32.
59. Nader A, Zahran N, Alshammaa A, Altaweel H, Kassem N, Wilby KJ. Population pharmacokinetics of intravenous methotrexate in patients with hematological malignancies : utilization of routine clinical monitoring parameters. *Eur J Drug Metab Pharmacokinet*. 2017;42(2):221–8.
60. Faltaos DW, Hulot JS, Urien S, Morel V, Kaloshi G, Fernandez C, et al. Population pharmacokinetic study of methotrexate in patients with lymphoid malignancy. *Cancer Chemother Pharmacol*. 2006;58(5):626–33.
61. Aquerreta I, Aldaz A, Giráldez J, Sierrasesúmaga L. Pharmacodynamics of high-dose methotrexate in pediatric patients. *Ann Pharmacother*. 2002;36(9):1344–50.
62. Odoul F, Le Guellec C, Lamagnère JP, Breilh D, Saux MC, Painaud G, et al. Prediction of methotrexate elimination after high dose infusion in children with acute lymphoblastic leukaemia using a population pharmacokinetic approach. *Fundam Clin Pharmacol*. 1999;13(5):595–604.
63. Crews KR, Liu T, Rodriguez-Galindo C, Tan M, Meyer WH, Panette JC, et al. High-dose methotrexate pharmacokinetics and outcome of children and young adults with osteosarcoma. *Cancer*. 2004;100(8):1724–33.
64. Borsi JD, Schuler D, Moe PJ. Methotrexate administered by 6-h and 24-h infusion: a pharmacokinetic comparison. *Cancer Chemother Pharmacol*. 1988;22(1):33–5.
65. Martelli N, Mathieu O, Margueritte G, Bozonnet MC, Daurès JP, Bressolle F, et al. Methotrexate pharmacokinetics in childhood acute lymphoblastic leukaemia: a prognostic value ? *J Clin Pharm Ther*. 2011;36(2):237–45.
66. Tiwari P, Thomas MK, Pathania S, Dhawan D, Gupta YK, Vishnubhatla S, et al. Serum creatinine versus plasma methotrexate levels to predict toxicities in children receiving high-dose methotrexate. *Pediatr Hematol Oncol*. 2015;32(8):576–84.
67. Reiss SN, Buie LW, Adel N, Goldman DA, Devlin SM, Doucer D. Hypoalbuminemia is significantly associated with increased clearance time of high dose methotrexate in patients being treated for lymphoma or leukemia. *Ann Hematol*. 2016;95(12):2009–15.
68. Relling MV, Fairclough D, Ayers D, Crom WR, Rodman JH, Pui CH, et al. Patient characteristics associated with high-risk methotrexate concentrations and toxicity. *J Clin Oncol*. 1994;12(8):1667–72.
69. Rau T, Erney B, Göres R, Eschenhagen T, Beck J, Langer T. High-dose methotrexate in pediatric acute lymphoblastic leukemia: impact of ABCC2 polymorphisms on plasma concentrations. *Clin Pharmacol Ther*. 2006;80(5):468–76.
70. Reeves DJ, Moore ES, Bascom D, Rensing B. Retrospective evaluation of methotrexate elimination when co-administered with proton pump inhibitors. *Br J Clin Pharmacol*. 2014;78(3):565–71.